Hindawi
Geofluids
Volume 2022, Article ID 2067228, 11 pages
https://doi.org/10.1155/2022/2067228

Research Article

Study on Pore Structure and Fractal Characteristics of Tar-Rich Coal during Pyrolysis by Mercury Intrusion Porosimetry (MIP)

Zhendong Wang,[1,2] Pengfei Jiang,[1,2,3] Fu Yang,[1,2] Yuanyuan Kong,[4] Li Ma,[1,2] Bohan Xie,[4] and Zhonghui Duan[1,2]

[1]*Key Laboratory of Coal Resources Exploration and Comprehensive Utilization, Ministry of Natural Resources, Xi'an 710021, China*
[2]*Shaanxi Coal Geology Group Co., Ltd, Xi'an 710021, China*
[3]*College of Geology and Environment, Xi'an University of Science and Technology, Xi'an 710054, China*
[4]*School of Highway, Chang'an University, Xi'an 710064, China*

Correspondence should be addressed to Pengfei Jiang; jiangpf@xust.edu.cn

Received 27 May 2022; Revised 29 July 2022; Accepted 23 August 2022; Published 7 October 2022

Academic Editor: Dengke Liu

This study aims to show how fractal analysis can be effectively used to characterize the pore structure of porous tar-rich coal. In this study, tar-rich coal pores were obtained by mercury intrusion porosimetry (MIP). The results showed that the sample had a high porosity and large pore diameter after pyrolysis, and the porosity of tar-rich coal was more than 35% at 600°C. The pore-throat ratio at high temperature was large, resulting in the high mercury retention rate. The pore distribution curves of samples at pyrolysis temperatures of 500 and 600°C were unimodal, and those of samples at room temperature and 150, 300, and 400°C were bimodal. The models for calculating fractal dimension based on MIP include Menger sponge model and thermodynamic model. Experiments show that the Menger sponge method is more reasonable when the pore size is less than 50 μm and greater than 350 nm. For the fractal dimension calculation of the whole pore curve section, the thermodynamic method was more reasonable. The use of fractal analysis in conjunction with the results of classical characterization methods leads to a better understanding of pore evolution in the pyrolysis process of tar-rich coal. The average fractal dimension could also be used as a valid parameter to monitor the textural evolution of the coals.

1. Introduction

Coal has an irreplaceable position in the world energy supply. In China, the energy structure is not extremely balanced, which is rich coal and less oil and gas. In 2017, coal accounted for more than 60% of China 's total energy consumption, but more than 80% of them were directly burned, and the utilization rate of coal was low [1, 2]. At the same time, it also brought serious environmental problems caused by excessive pollutant emissions, such as greenhouse effect, acid rain, and haze weather. Therefore, an effective way of improving economic efficiency and solving environmental problems is to make full use of coal [3, 4].

In recent years, tar-rich coal has been recognized as a special kind of coal resource. Tar-rich coal is a kind of coal with oil content of 7%~12%. More than half of China 's coal reserves belong to high tar-rich coal. The formation of tar-rich coal has a specific geological historical evolution process and geological accumulation conditions. The tar yields of tar-rich coals in different ages, different regions in the same age, and different stratum in the same age are significantly different [5]. More than 150 billion tons of tar-rich coal have been discovered in the northern Shaanxi Province, China, where 14.5 billion tons of oil can be exploited from the tar-rich coal as an important supplementary energy.

Tar in coal can be extracted by low-temperature pyrolysis. In the previous development and utilization of coal, the using of tar-rich coal as ordinary coal results in a large waste of energy resources. The pyrolysis technology of tar-rich coal can be divided into two ways. One way is ground pyrolysis which belongs to the ectopic pyrolysis method after mining. Another way is in-situ pyrolysis, which has great potential

for green and low-carbon development, and it can achieve the purpose of "extracting hydrogen and fixing carbon" [6, 7]. In the in-situ pyrolysis process, by drilling into the coal seam, and then using the wellbore as a channel, the coal seam is heated to the pyrolysis temperature in a certain way. Therefore, oil and gas generate, and are collected from the ground by conventional methods. The advantage of underground in situ pyrolysis of coal is to make most of the carbon in coal to remain in the residual coke [8]. Tar-rich coal after in situ pyrolysis can still be exploited as conventional coal in the later stage, and higher calorific values can be obtained.

Pores are important channels for coal tar migration, especially the connected pores. The connected pores are usually large pores [9], and large pores with good connectivity can ensure the timely discharge of tar and improve the pyrolysis efficiency of coal samples [10, 11]. In addition, pores with good connectivity can accelerate the pyrolyzation and ensure the rapid pyrolysis of coal samples [12]. Previous studies focus on the pore structure characteristics of coal at ambient temperature, which was used to analyze gas migration in the coal seam. Coal matrix structures and pores in these structures can be characterized by various methods, such as CT scanning, nuclear magnetic engineering, nitrogen adsorption method, scanning electron microscopy, and mercury injection [5]. During the pyrolysis of tar-rich coal, pyrolysis pores generate continuously due to the pyrolysis of organic matter components. The pore structure is constantly changing to be complex and irregular. The variation of pore structure not only affects the physical properties of tar-rich coal, but also impacts on the migration of pyrolysis products [12, 13]. Determining the evolution process of pore structure is of great significance to clarify the in situ pyrolysis mechanism and the generation of pyrolysis products.

The purpose of this study is to analyze the effect of temperature on tar-rich coal pyrolysis pore structure. MIP test was done to acquire the pore characteristics with different pyrolysis temperatures. The fractal characteristics of the pores at different pyrolysis temperatures were obtained. Analyzing the effect of temperature on coal pyrolysis pores is conducive to study the conditions for making full use of tar-rich coal energy. It can provide a theory basis for further study of hydrocarbon migration during in situ pyrolysis of tar-rich coal.

2. Experimental and Theory

2.1. Samples. The tar-rich coal samples studied were collected from Xiaobaodang Coal Mine, located in Yulin City, northern Shaanxi Province, China. The samples were selected at a depth of 400 m as the studied tar-rich coal. The coal samples presented black and brown when they were extracted as complete blocks. The samples were analyzed by proximate analysis, ultimate analysis, and Gray-King assay analysis. Table 1 shows the results.

To study the evolution characteristics of the pore structure of tar-rich coal samples during pyrolysis, a tube furnace was used to heat tar-rich coal block (about 20 g) samples to 200°C, 300°C, 400°C, 500°C, and 600°C, respectively, in nitrogen atmosphere. The samples were kept for two hours at a predetermined temperature and then were cooled down naturally. Until it reached to room temperature, the block samples were taken out from the tube furnace, respectively, named S2-S6. The normal temperature sample was named S1. Six tar-rich coal samples were processed into 1~2 g blocks for later MIP test to detect the pore characteristics. Some coal samples of S1 were crushed to 80 mesh for thermogravimetric analysis.

2.2. Thermogravimetric Analysis. The thermogravimetric analysis was carried out to analyze the pyrolysis behavior of coal samples. The instrument used for the test was Netzsch STA 449C (Germany) thermal analyzer. 5 mg sample was heated to 800°C with a heating rate of 10°C/min. High purity nitrogen was used as the sweeping gas, the flow rate maintained at 80 ml/min.

2.3. MIP Test and Theory. The MIP test was performed using a Micromeritics Instrument Corporation AutoPore V 9600 (USA). The S1-S6 block samples used for the MIP were dried under vacuum at 80°C for 24 h. The maximum working pressure of the instrument was 33,000 psi (227 MPa). The pressure was gradually reduced to atmospheric pressure at the end of the mercury intrusion test. Pressure and mercury volume were recorded during the test. Pore diameter under the corresponding pressure can be calculated by Washburn Formula (1) [14].

$$p = -\frac{2\gamma \cos\theta}{r}. \tag{1}$$

The surface tension γ of mercury is set to 0.485 N/m; the contact angle θ is 130°, and the corresponding pore size is calculated to be 5 nm-120 um.

Since the porous nature of coal is important in its handling, preparation, and utilization, much effort is expended in the measurement of the pore size distribution. During MIP test, the pore throat in the sample resembles a capillary tube, and the mercury is subjected to capillary pressure during both intrusion and extrusion. In the mercury intrusion process, the capillary pressure is the resistance of the mercury to enter the sample pores, and during mercury extrusion, the capillary pressure is forcing the mercury to exit from the sample pores.

Recent work has shown that fractal geometry provides a useful description of porous surfaces by characterizing the pore size distribution over a range of pore sizes by a single quantity, the fractal dimension D. The fractal dimension was determined from the relation $dV_p/dP \propto p^{D-4}$, where P is the pressure [15].

2.4. Fractal Dimensional Theory. Numerous studies showed that the pore structure of tar-rich coal was complex and the surface morphology was irregular [12]. It has obvious self-similarity in a certain scale range, which presents a fractal feature. The spatial morphology is between two and three dimensions, which is difficult to characterize by the traditional Euclidean geometry methods. The fractal dimension

Table 1: Basic properties of tar-rich coal.

Proximate analysis (wt%)				Ultimate analysis (wt%)				Gray-king assay analysis (wt%)			
Moisture	Ash	Volatile	Fixed carbon	C	H	N	S	Tar	Gas	Water	Semicoke
6.78	8.45	36.58	48.19	76.02	5.08	0.75	0.52	9.08	8.57	9.98	72.37

is a significant parameter to quantitatively characterize the fractal of porous medium, reflecting the nonhomogeneity of the pore structure and the complexity of the surface. The models for calculating fractal dimension based on mercury intrusion method include Menger sponge model and thermodynamic model.

2.4.1. Menger Sponge Model. The reasonable range of fractal dimension of tar-rich coal sample pores is 2-3. The larger the fractal dimension is, the closer it is to three-dimension; the more complex the pore structure is, the rougher the pore surface is. The Menger sponge model is used to calculate the fractal dimension of tar-rich coals at different pyrolysis temperatures, because it simulates the pore structure and the coexistence of pore sizes at various levels, and can provide a complete and continuous characterization of pore sizes at various spatial scales [16]. Using the incoming mercury pressure and the accumulated incoming mercury volume of the press through process, the specific expression of the model is as follows [17]:

$$\ln\left(\frac{\mathrm{d}V}{\mathrm{d}P}\right) = (D-4)\ln P + C, \tag{2}$$

where P is the mercury intrusion pressure/Pa, V is the accumulated mercury injection volume (m^3) at mercury intrusion pressure P, D is the fractal dimension, and C is constant.

The slope of the fitted line based on ln $(\mathrm{d}V/\mathrm{d}P)$ and ln (P) is $(D-4)$, therefore, the fractal dimension can be calculated by the slope plus 4.

2.4.2. Thermodynamic Model. During the mercury injection process of MIP, as the pressure p applied to the mercury from outside increases, the volume of mercury entering the pores of the tar-rich coal increases, and the surface energy of the system increases. The work done by the external environment on mercury is equal to the incremental surface energy of the mercury entering the pore space. Combining the equation given by Mandelbrot for the surface area of the fractal and its pore volume, the equation that should be satisfied by the pressure p (applied to the mercury) and V (the volume of mercury intrusion) in the MIP is finally obtained as follows [18]:

$$\sum_{i=1}^{n} \overline{P_i}\Delta V_i = K r_n^2 \left(V_n^{1/3}/r_n\right)^{\mathrm{D}_T}, \tag{3}$$

where $\overline{P_i}$-average pressure of the ith mercury intrusion operation kPa; ΔV_i is the amount of mercury volume in the ith mercury intrusion operation, cm^3/g; n- number of pressure intervals applied in the mercury intrusion operation; r_n is the pore radius corresponding to the nth mercury intrusion, nm; V_n the cumulative amount of mercury intrusion at a pressure interval of n, cm^3/g; D_T is the fractal dimension based on the thermodynamic model; K is the parameter.

Make

$$W_n = \sum_{i}^{n} \overline{P_i}\Delta V_i, \quad Q_n = V_n^{1/3}/r_n. \tag{4}$$

Q_n *is* the function of pore radius r_n and pore volume V_n at the nth stage of the mercury intrusion process [17].

Substituting into Equation (3) and taking the logarithm of both sides yields:

$$\lg\left(W_n/r_n^2\right) = \mathrm{D}_T \lg Q_n + \mathrm{C}. \tag{5}$$

From Equation (5), it can be seen that the thermodynamic fractal dimension D_T can be obtained by fitting the data of the mercury intrusion process in the MIP with lg (W_n/r_n^2) and lgQ_n as the vertical and horizontal coordinates, and finding the slope of the fitted line is D_T.

3. Results

3.1. Pyrolysis Behavior and Characteristics. As shown in Figure 1, the curve is obtained from the thermogravimetric analyzer. Figure 1 shows the TG and DTG curves of S1. It can be seen from the TG curve that the maximum mass loss of the samples was about 35%. The whole process of pyrolysis process of tar-rich coal was basically divided into three sections according to the DTG curve. The first segment was in a temperature range below 250°C, and the mass loss at this stage is mainly caused by the evaporation of water in the sample. The second stage was in the temperature range of 250°C-650°C. This stage was the main weight loss stage, caused by the pyrolysis and volatilization of organic matter in the sample. Oil and gas production began in this stage. When the temperature was above 650°C, the tar-rich coal still has little mass loss, mainly caused by the decomposition of mineral composition or the loss of bounding water. The maximum mass loss rate of tar-rich coal pyrolysis occurred at the temperature about 460°C. When the temperature is higher than 650°C, the mass loss is small, indicating that the sample pyrolysis is basically complete. The mass loss can be seen from the TG curve. At a certain temperature, when the mass loss is constant, the tar-rich coal is basically completely decomposed.

3.2. Evolution Characteristics of Pore Structure in the Pyrolysis Process

3.2.1. Pore Size and Porosity Evolution Characteristics. The mercury intrusion and extrusion curves of S1-S6 measured by MIP are shown in Figure 2. It can be seen from the curves that the cumulative mercury intrusion of S1-S3 was

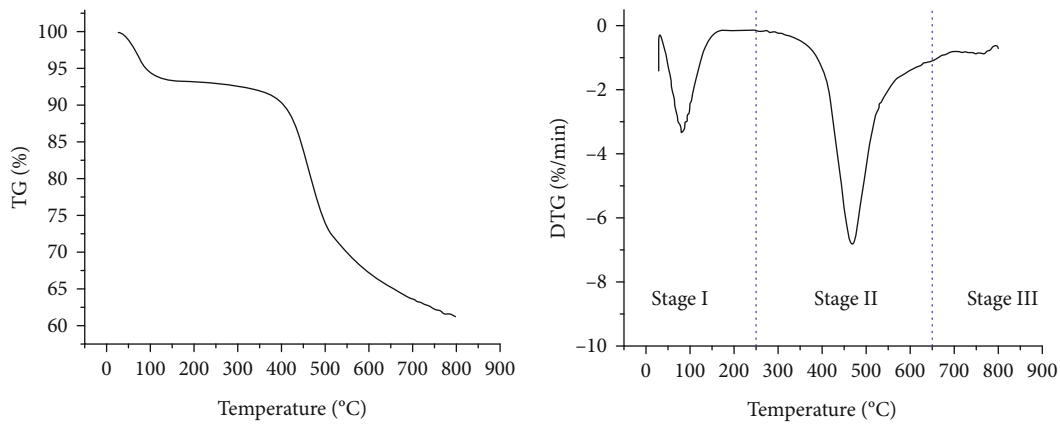

Figure 1: TG and DTG curve of tar-rich coal.

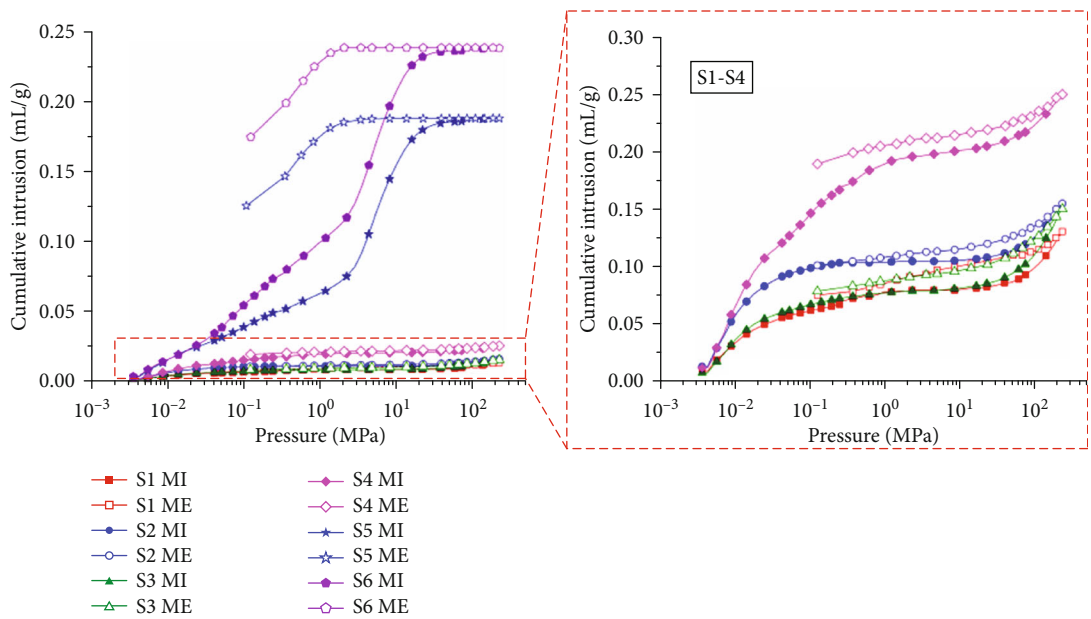

Figure 2: Mercury intrusion and extrusion curves of S1-S6 samples (MI-Mercury intrusion and ME-Mercury extrusion).

relatively small at about 0.02 mL/g. The cumulative mercury intrusion of S4 sample slightly increased to 0.025 mL/g, while that of S5-S6 was above 0.2 mL/g, indicating that pyrolysis pores began to form at 400°C. A large number of pyrolysis pores were generated in the samples within 500°C to 600°C, which was consistent with the results of thermogravimetric analysis.

Because the porosity of coal is measured by MIP. The percentage of each type of pore is shown in Table 2. High-pressure mercury injection test cannot characterize submicropores with pore size less than 5 nm (Pores less than 5 nm are submicropores). Hodot classification method was introduced to classify the nanoscale pores of tar-rich coal into: submicropore (<5 nm), micropore (5 nm-10 nm), transition pore (10 nm-100 nm), mesopore (100 nm-1000 nm), and macropore (>1 000 nm) ([19, 20]). At the same time, the pores are divided into seepage pores (>100 nm) and diffusion pores (<100 nm). According to IUPAC classification standard, coal pores can be divided into micropore (<2 nm), mesoporous (2 nm-50 nm), and macropore (>50 nm). Nitrogen adsorption experiment can be used to determine this part in the further work.

Table 2: Nanoscale pore classification of tar-rich coal.

Pore type	Pore size (nm)	Pore type	IUPAC pore size (nm)
Submicropore	<5	Micropore	<2
Micropore	5~10	Mesoporous	2~50
Transition hole	10~100		
Middle hole	100~1000	Macropore	>50
Macropore	>1000		

As shown in Figure 2, the mercury injection curves of S1-S6 differed greatly and can be basically divided into two types. The first type had a large total mercury intake, such

as the mercury injection curves of S5 and S6 and had a large volume difference between mercury injection and extrusion, and the pore hysteresis loops were wide. However, the mercury retention ratios of S5 and S6 were high, reaching 73.2% and 75.7%, respectively. This indicated that when the pyrolysis temperature was high (500-600°C), the sample had a high porosity and large pore diameter. However, the pore-throat ratio of S5 and S6 was big (Figure 3), resulting in the high mercury retention rate.

In the second type, the pore hysteresis loops of mercury injection curves were narrow, the volume difference between mercury intake and extrusion was small. There was sectional coincidence of mercury injection and ejection curves. The mercury retention ratios of S1-S4 samples were 57.5%, 61.3%, 53.4%, and 66.6%, respectively. With the increase of pyrolysis temperature, the mercury retention ratio of samples gradually raised. The high retention volume was indicative of the existence of throats in the pore network.

The ratio of the volume of retained mercury to the total volume of mercury intrusion is the mercury retention rate. Pore-throat ratio denotes the ratio of pore body size to pore throat size at the same mercury saturation, as shown in Figure 3 [21–23]. High mercury retention indicated poor pore connectivity, and the mercury retention was positively correlated with the pore-throat ratio. It can be seen from Figure 3 that the pore-throat ratio became higher when the pyrolysis temperature was 500-600°C. The pore connectivity increased with the mercury retention reducing, and it was concluded that the pore connectivity of tar-rich coal was the best within 200-300°C.

The porosity and pore diameter were linearly fitted as shown in Figure 4(a). It can be seen that porosity was positively correlated with both median pore diameter and average pore diameter. The increase of porosity mainly comes from the contribution of large diameter pores. The porosity and pore diameter curves obtained by MIP are shown in Figure 4(b).

The porosity of S6 reached 35% and had the largest pore diameter. The average pore diameter increased from 20 nm to 240 nm, and the median pore diameter increased from about 10 nm to 100 nm. Indeed, the pyrolysis resulted in a lot of changes in the pore structure. Pyrolysis volatilization of organic matter composition produced a large number of pores with different pore diameters. This created conditions for the pyrolysis products to percolate in the pores of tar-rich coal.

Mercury retention was positively correlated with pore size (Figure 5). Although the average pore diameter of S5 and S6 was large, the mercury retention rates remained high. 12.The large mercury retention rate meant the existence of throats in the pore network. The pore-throat ratio also changed regularly with the increase of pyrolysis temperature (as shown in Figure 3). In addition, the pore-throat ratio reflected the seepage characteristics of the pores clearly. The high pore-throat ratios were related to the products at different temperature stages in the pyrolysis process of tar-rich coal. It can be seen from Figure 3 that in the seepage range, the pore-throat ratio changed with the increase of

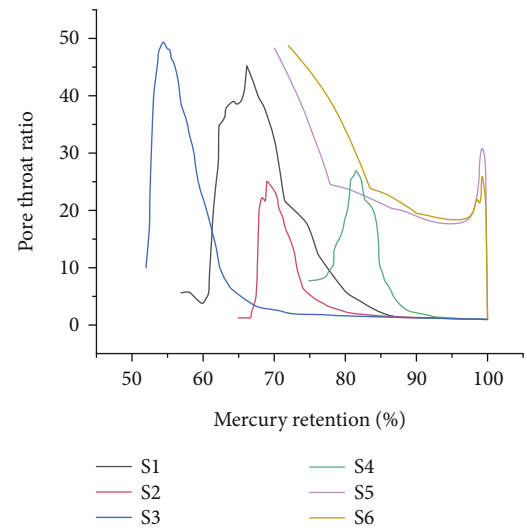

Figure 3: Curves of pore-throat ratio and mercury retention rate.

mercury retention, showing a single peak. The mercury retention was mainly related to pore-throat ratio. There is a positive correlation between mercury retention rate and pore size. As the temperature rose, more oil and gas substances were produced, resulting in a large number of pores. Some substances solidified with the temperature rising, resulting in pore throat blockage, so the mercury retention rate was higher.

3.2.2. Pore Distribution Characteristics. The pore distribution diagrams were summarized according to the MIP results. As shown in Figure 6, the evolution characteristics of pores in tar-rich coal at different pyrolysis temperatures were observed.

The pore distribution of S1 samples presented a bimodal phenomenon, that is, a high peak occurred in two pore sizes of "near 10 nm" and "near 1000 nm", explaining that tar-rich coals in the study area mainly developed micropores and macropores. The pore distribution diagrams at different pyrolysis temperatures were observed. S2-S4 diagrams showed bimodal characteristics, but S5 and S6 showed unimodal characteristics.

The porosity showed an increasing trend with the increase of average pore diameter. The proportion of micron pores gradually decreased, which indicated that the porosity of each sample was mainly contributed by the micron pores. The retention of mercury basically enlarged with the increase of average pore diameter, indicating that mercury was mainly retained in the micron pores. Therefore, the poor connectivity of micron pores was related to the intergranular pores of minerals in the sample, and affected by the products generated during pyrolysis [24].Through the glass tube simulation ink bottle pore throat structure research, with the increase of pore throat ratio, mercury retention also increased ([25]). The more developed the micron pores, the larger the average pore-throat ratio, the larger the mercury retention, and the worse the pore connectivity; the more developed the nanopores, the smaller the

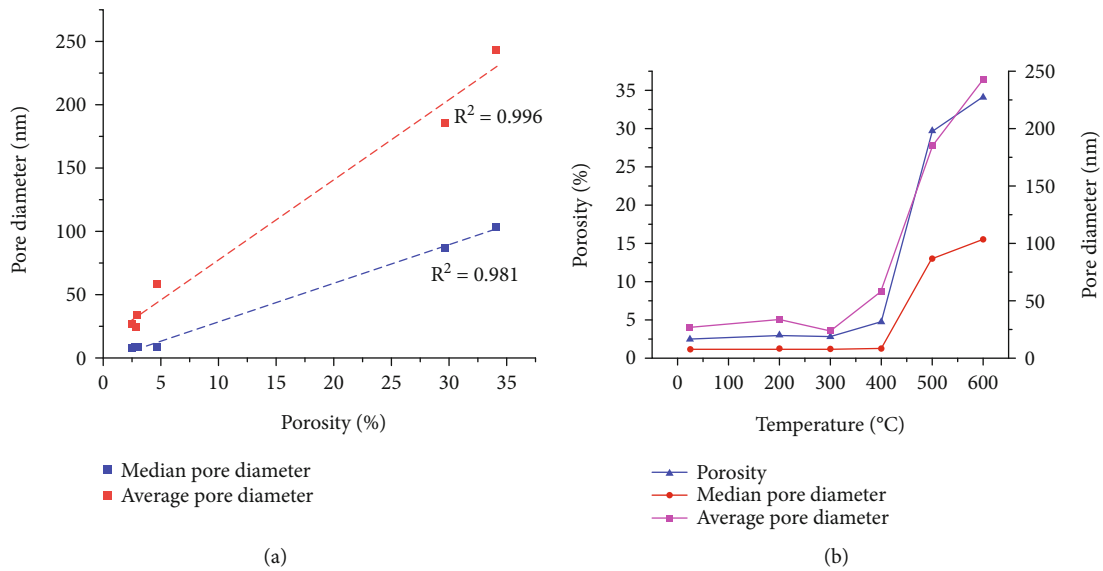

Figure 4: Curves of the porosity and pore parameters: (a) Fitting curves of porosity and pore size; (b) Curves of porosity and pore diameter change with pyrolysis temperature.

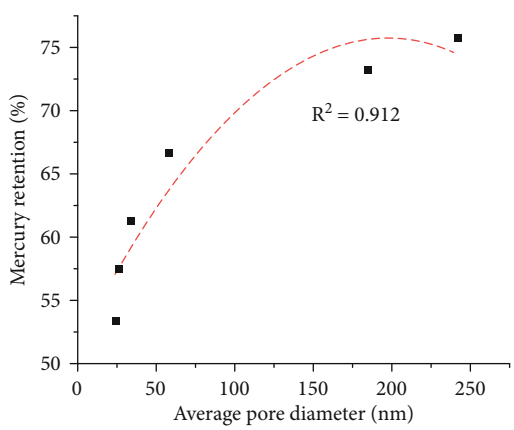

Figure 5: Curves of the mercury retention and average pore diameter.

average pore throat ratio, the smaller the mercury retention, and the better the pore connectivity [26].

3.3. Fractal Characteristics of Tar-Rich Coal

3.3.1. Fractal Characteristics Obtained by Mengel Sponge Model. According to MIP data, the coal pore structure fractal characteristic curves of S1-S6 were shown in Figure 7. The fractal characteristic curves of S1-S6 were clearly segmented. The fractal characteristic curve of each sample can be divided into two sections for linear fitting, respectively, which were denoted as the low-pressure section fractal dimension D1 and high-pressure section fractal dimension D2.

When the mercury injection pressure was less than 3.27 MPa, the fractal dimension D1 increased as the temperature increased in the range of normal temperature to 400°C. When the temperature was greater than 400°C, the fractal dimension D1 of S6 was gradually going up to 3.09, but the fractal dimension D2 of the high-pressure section reduced gradually with the increase of temperature. However, when the mercury injection pressure was greater than 3.27 MPa, the fractal dimension D2 greatly increased, even exceeding 4. The fractal dimensions calculated by this method in the high pressure stage of S1-S4 samples were greater than 3, noting that this method was not suitable for the calculation of the pore fractal dimension in the high pressure section.

3.3.2. Fractal Characteristics Obtained by Thermodynamic Method. By fitting the MIP data of S1-S6, the slope of the fitting line can be calculated, which is the fractal dimension obtained by thermodynamic method. The results are shown in Figure 8. The fractal dimensions of S1 to S6 were 2.559, 2.516, 2.593, 2.507, 2.620, 2.590, respectively. The values of the fractal dimensions were all between 2 and 3, and the calculated results were reasonable.

4. Analysis and Discussion

4.1. Pore Structure Evolution of Tar-Rich Coal. In the process of low temperature distillation of tar-rich coal, the oil and gas production can be divided into the following stages [27]:

Stage I: in the range of 100~200°C, the sample was dried, carbon dioxide and methane adsorbed in coal pores were precipitated.

Stage II: when the temperature raised to 200-350°C, the coal began to decompose. At this time, the side chains in the coal structure started to break down, mainly producing pyrolytic water, carbon dioxide, carbon monoxide, methane, and other gases, and tar began to escape.

Stage III: in the range of 350~480°C, the colloids formed. Side chains in the coal macromolecules further decomposed to form a large amount of viscous liquid, in which there were also gas bubbles, and the remains of coal particles that had not completely decomposed. This liquid-based colloid

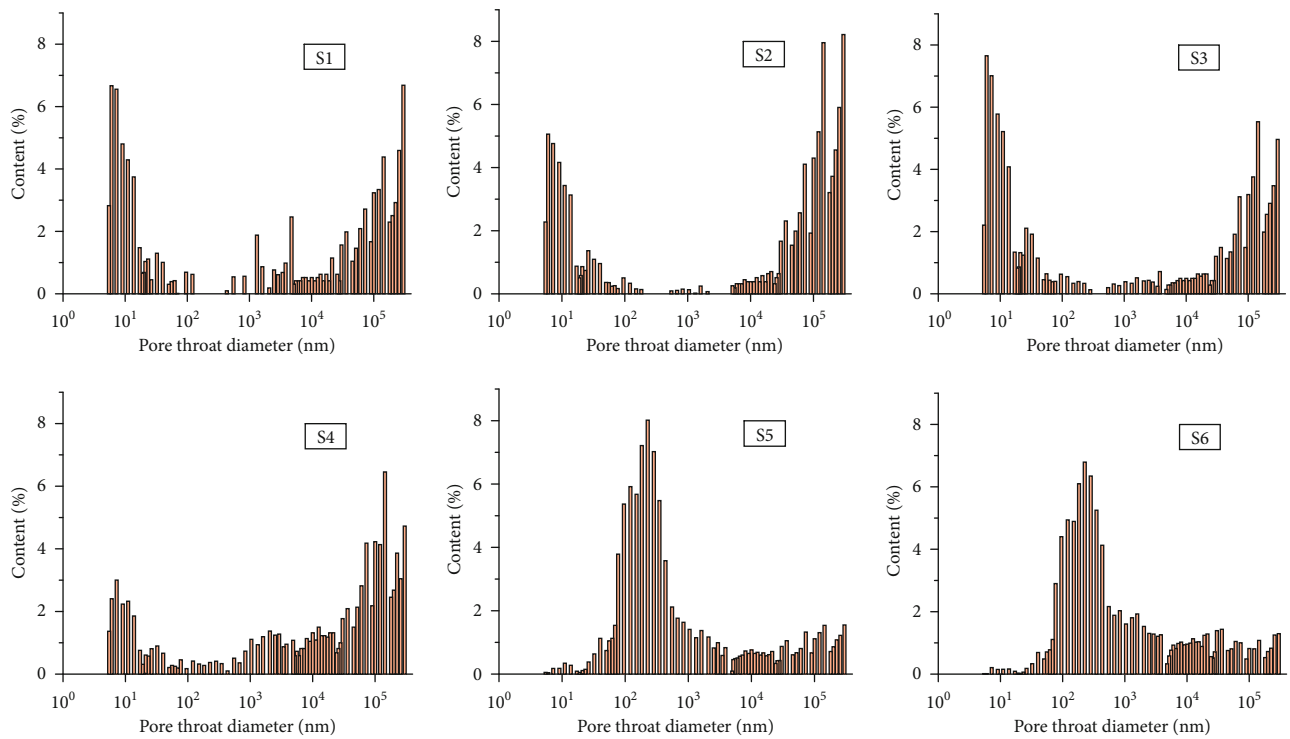

Figure 6: Diagram of various pore contents of tar-rich coal after pyrolysis.

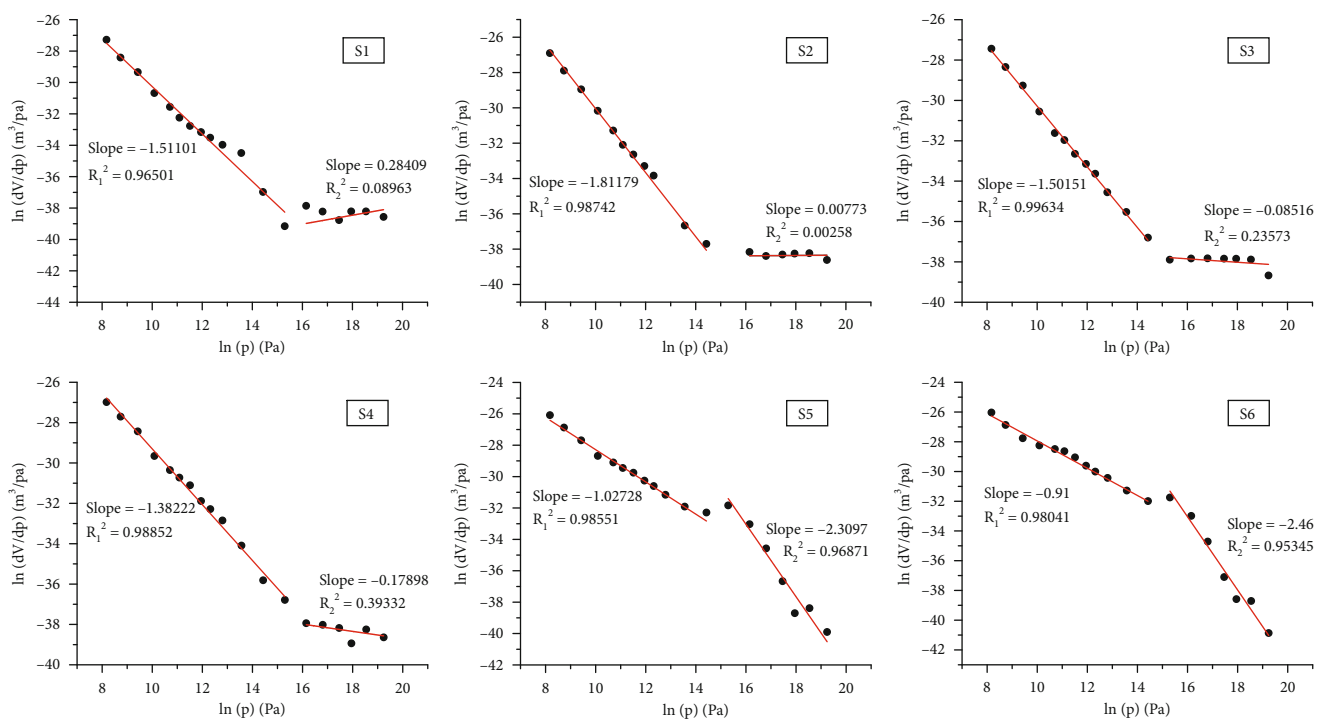

Figure 7: Fractal dimension of pores calculated by Menger sponge method.

system consisting of gas, liquid, and solid phases becomes a colloid with adhesive properties. Because the gelatinous body was not breathable, the expansion pressure was generated. At this stage, large quantities of gaseous and liquid products were produced.

Stage IV: in the range of 480~550°C, the liquid in the colloidal body was further decomposed. Part of that was precipitated in gaseous form and part solidified into semi-coke. Large amounts of gaseous products continued to be produced, while tar escape gradually decreased.

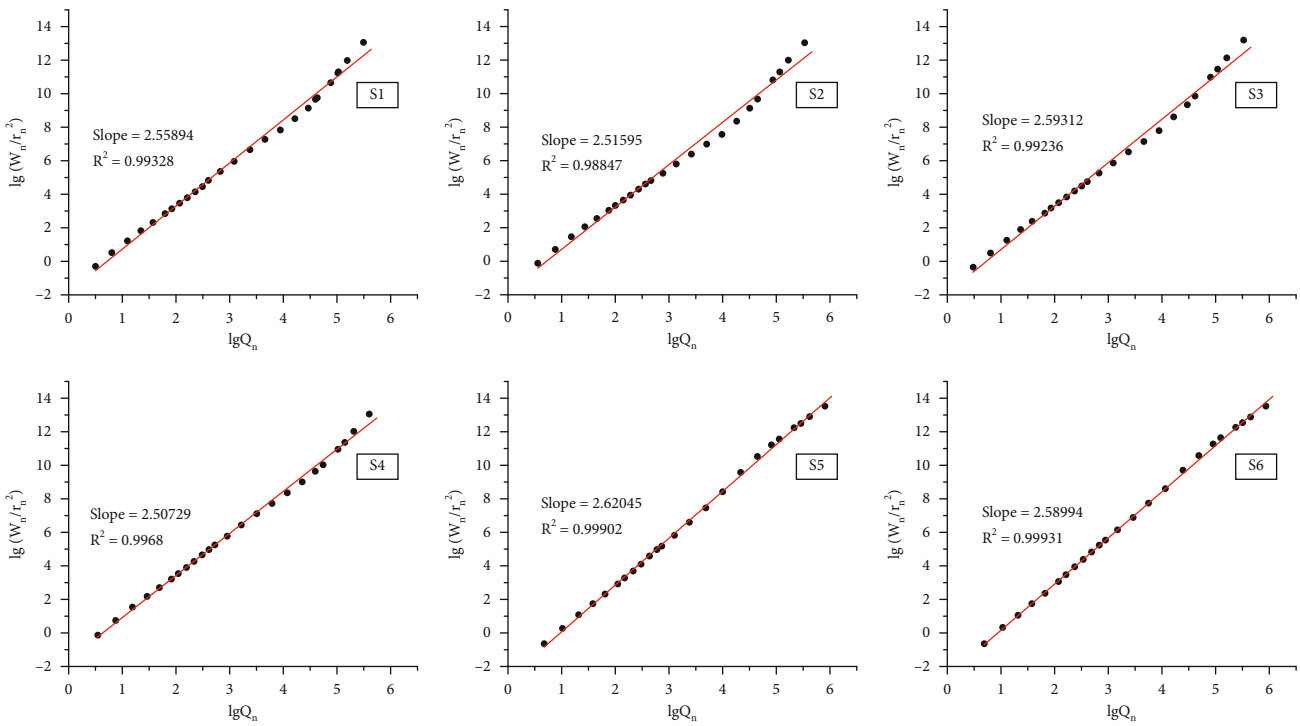

Figure 8: Fractal dimension of pores calculated by thermodynamic method.

Stage V: when the temperature was greater than 550°C, the tar stopped escaping. Semicoke contraction occurred in this stage, resulting in coke formation. And numerous fissures were formed in the coal.

Figure 9 shows SEM images of samples heated to 600°C and 300°C. The SEM image of 600°C displayed massive micro cracks forming on the bedding surface of tar-rich coal, the size of the cracks and pores could reach 2-8um. The SEM image of 300°C presented the micro stratification development of tar-rich coal. Although the porosity increased clearly during the pyrolysis process, the volume of coal tended to expand due to the cracking evolution on the bedding surface and expansion cracking between stratifications. This was the cause of coal volume increase after heating.

In the evolution of gas coal pyrolysis fracture pores, it was easy to pyrolyze. At 200°C, new pores were generated due to the pyrolysis of gas coal. It could be clearly seen that these new pores are mainly round and oval, and the edge of the pores is relatively smooth. At 500°C, tar-rich coal started to rapidly pyrolysis and produce a large number of pores, and the pore shape was mostly round and oval [28].

Table 3 shows the various pore contents of S1 and S6. Seepage pores referred to the medium and large pores with pore sizes greater than 100 nm. The proportion of seepage pores improved gradually with the increase of pyrolysis temperature.

The pores of S1-S6 produced distinct evolution characteristic at different pyrolysis temperature stages due to the change of pyrolysis production. In the range of diffusion pore (<100 nm) diameter, the pore-throat ratios of S5 and S6 were close to 20; In the range of seepage pores (>100 nm), the pore-throat ratio maximum values of S5 and S6 were nearly 60 and 50, respectively [29].

The colloid formed in this stage flowed, and these substances partially filled the pores, making the pores surface smoothly. The fractal dimension was calculated by the thermodynamic method, and the fractal dimension of S4 was the smallest, indicating that the complexity of pore structure reduced due to the flowing and coverage of colloid. The results manifested the maximum mass loss rate of tar-rich coal pyrolysis occurred in this stage. A large amount of gas-liquid products was produced, and the porosity of the sample began to increase greatly at this stage. The throat of diffusion pores was large, while the throat of seepage pores was small.

In stage IV, a large amount of gaseous substances formed and escaped, which led to dramatic changes in pore structure and high porosity. In the previous stage. Part of the colloidal substances solidified to form semicoke, resulting in an increase in the pore throat ratio of seepage pores. Due to the formation of semicoke, the fractal dimension of the pores became larger, and the proportion of seepage pores increased to 83%. When the pore diameter was large but the pore throat was small, that would lead to a high mercury retention rate. In essence, a high pore throat ratio was not conducive to oil and gas seepage and migration during pyrolysis.

The pore size distribution of the samples in the low pressure range ($0.003\,\text{MPa} < p < 0.95\,\text{MPa}$) was between 1300 nm and 352000 nm, which belonged to macropores and macrocracks. The pore throat ratios of S1-S4 samples were small in the range of large pore size.

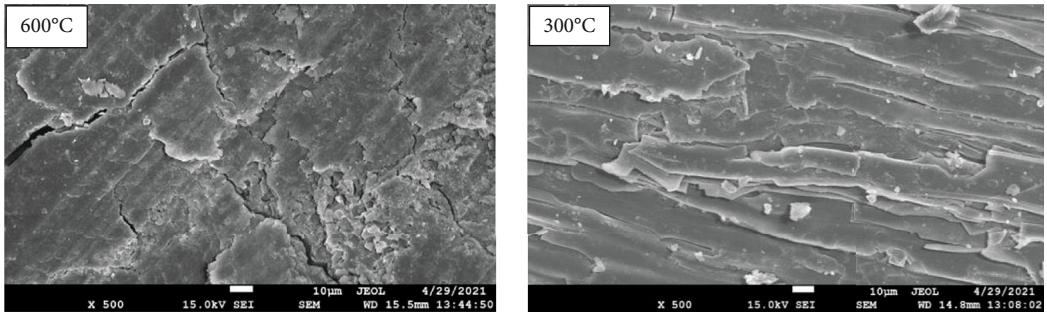

Figure 9: SEM images of samples heated to 600°C and 300°C.

Table 3: Various pore contents of tar-rich coal after pyrolysis/%.

Pore size range/nm	S1	S2	S3	S4	S5	S6
Micropore (5-10)	25.5	19.9	23.4	9.3	0.5	0.4
Transition pore(10-100)	13.5	12.4	22.7	9.9	16.5	12.2
Medium pore (100-1000)	2.1	1.2	3.2	4.7	49.6	46.1
Large pore (>1000)	58.9	66.5	50.7	76.1	33.4	41.3
Diffusion pore (<100)	39.0	32.3	46.1	19.2	17.0	12.6
Seepage pore (>100)	61.0	67.7	53.9	80.8	83.0	87.4

Table 4: Fractal dimensions of S1-S6.

Method	Type	S1	S2	S3	S4	S5	S6
Menger sponge model	D1	2.49	2.19	2.50	2.62	2.97	3.09
	D2	4.28	4.01	3.92	3.82	1.69	1.54
Thermodynamic method	D_T	2.56	2.52	2.59	2.51	2.62	2.59

4.2. Fractal Dimensions of Tar-Rich Coal. In this experiment, all pores larger than 0.5 nm could be detected, but not all pores in all pore sizes had fractal characteristics, or the fractal dimensions in different apertures represented different physical or mechanical mechanisms [30]. Table 4 shows the fractal dimensions of S1-S6. The fractal dimensions were calculated by Menger sponge model subsection. It was irrational that the pore fractal dimension D2 at high pressure section was greater than 3 or less than 2. Menger sponge model was not suitable for the calculation of high pressure section. The pore fractal dimension at low pressure section was basically between 2 and 3, which was reasonable. Generally, the data of the initial pressure and high pressure sections would be excluded when calculating the fractal dimension of mercury injection. The reasons were as follows: at low pressure, the behavior of mercury just pressing into the coal pores did not conform to the fractal law in nature; however, at high pressure, the coal was a high elastic body; the pore fractal dimension reflected the compression behavior of coal to a certain extent, and it wasn't completely the pore fractal dimension. In this paper, the fractal method obtained through Menger sponge model did not reflect the fractal characteristics of pores with aperture less than 350 nm. The fractal dimension $D1$ value of S6 was greater than 3 by this method, which was beyond the significance of the pore fractal dimension [31–33]. The results above expounded when the tar-rich coal was heated to 600°C; the coal was filled with various pores and microcracks, resulting in a very complex inner structure with a high pore throat ratio and poor pore connectivity.

The pore diameter in the range of 13.8 MPa was greater than 100 nm. The fractal dimension of the tar-rich coal seepage pores reflected the essential characteristics of the pore surface and pore structure of coal. By comparing the coals at different pyrolysis temperatures and analyzing the pore fractal dimension, we studied the pore variation law in the pyrolysis process, which was the essential reason for the obvious difference in the permeability of coals at different pyrolysis stages. The change of physical and chemical structure of coal caused the change of coal composition (such as moisture, ash, etc.) and pore structure, which further affected the fractal dimension of coal pores. Compared with the two methods, the fractal dimension calculated in the low pressure section was more reasonable. For the fractal dimension calculation of the whole pore curve section, the thermodynamic method was more reasonable.

5. Conclusions

The fractal dimension obtained by analyzing data from MIP was a useful parameter for the study of the pore structure of tar-rich coal. The pore distribution and fractal characteristic at different pyrolysis temperatures were obtained through the Menger sponge method and thermodynamic method. The results obtained lead to the following conclusions:

(i) after pyrolysis, the sample had a high porosity and large pore diameter. The porosity of tar-rich coal was 35% at 600°C. The pore-throat ratio at high temperature was large, resulting in the high mercury retention rate

(ii) the pore fractal dimension of tar-rich coal at different temperatures was calculated by Menger sponge method and thermodynamic method. The calculation of fractal dimensions at low pressure was more reasonable, that is, the fractal dimension of pores with pore diameter less than 50 μm and larger than 350 nm was more suitable by the first method. Applying thermodynamic methods, it was possible to estimate the overall fractal dimension for all pore size ranges studied, as the values lg (W_n/r_n^2) vs. lgQ_n could fit a straight line fairly well. The fractal dimension D_T were between 2 and 3

(iii) the pyrolysis process modified the fractal dimension of the pore network. The fractal dimension D1 at low pressure section decreased first and then increased with pyrolysis temperature increasing. However, the maximum mass loss rate of tar-rich coal pyrolysis occurred at the temperature about 460°C. The sample had a minimum fractal dimension D_T in stage III (350-480°C)

(iv) the features of conventional techniques of pore analysis are enhanced when used together with data proceeding from fractal analysis. The fractal dimension of a surface is an intrinsic characteristic of the said surface and is theoretically independent of its size or macroscopic shape. Due to this fact, the textural changes originated as a consequence of the pyrolysis process of tar-rich coal are better understood by combining fractal and traditional methods of analysis

Data Availability

The data used to support the findings of this study are included within the article.

Conflicts of Interest

The authors declare that they have no conflicts of interest.

Acknowledgments

This work was supported by the Key Scientific Research Project of Shaanxi Coal Geology (SMDZ-2020ZD-1); Shaanxi Province Young Science and Technology Nova Project (2022KJXX-24); the Qinchuangyuan Scientist & Engineer Team Project of Shaanxi Province.

References

[1] H. Zhao, L. Jin, M. Wang, B. Wei, and H. Hu, "Integrated process of coal pyrolysis with catalytic reforming of simulated coal gas for improving tar yield," *Fuel*, vol. 255, article 115797, 2019.

[2] B. Tian, Y. Qiao, Y. Tian, and Q. Liu, "Investigation on the effect of particle size and heating rate on pyrolysis characteristics of a bituminous coal by TG-FTIR," *Journal of Analytical and Applied Pyrolysis*, vol. 121, pp. 376–386, 2016.

[3] J. Wu, J. Liu, S. Yuan et al., "Sulfur transformation during hydrothermal dewatering of low rank coal," *Energy & Fuels*, vol. 29, no. 10, pp. 6586–6592, 2015.

[4] R. Yan, H. Zhu, C. Zheng, and M. Xu, "Emissions of organic hazardous air pollutants during Chinese coal combustion," *Energy*, vol. 27, no. 5, pp. 485–503, 2002.

[5] Y. Chen, C. Jiang, J. Leung, A. K. Wojtanowicz, and D. Zhang, "Multiscale characterization of shale pore-fracture system: geological controls on gas transport and pore size classification in shale reservoirs," *Journal of Petroleum Science and Engineering*, vol. 202, article 108442, 2021.

[6] S. Wang, Q. Shi, S. Wang, J. Shen, Q. Sun, and Y. Cai, "Resources property and explaitation concepts with green and low-carbon of tar-rich coal as coal-based oil and gas," *Journal of China Coal Society*, vol. 46, no. 5, pp. 1365–1377, 2021.

[7] Y. Yan-bin, L. Da-meng, H. Wen-hui, T. Da-zhen, and T. Shu-heng, "Research on the pore-fractures system properties of coalbed methane reservoirs and recovery in Huainan and Huaibei coal-fields," *Journal of China Coal Society*, vol. 31, no. 2, pp. 163–168, 2006.

[8] S. Ge, "Chemical mining technology for deep coal resources," *Journal of China University of Mining and Technology*, vol. 46, no. 4, pp. 679–691, 2017.

[9] G. Lu, S. Yang, Y. Zhang, Y. Wang, and Y. Zhao, "Pore structure characteristics and their controlling factors of sandstone reservoirs in the lower Xiaganchaigou formation in Mahaidong area," *Petroleum Geology & Oilfield Development in Daqing*, vol. 40, no. 2, pp. 20–29, 2021.

[10] M. Miao, "Influences of depositional environment on reservoir space of coal in Hegang coalfield," *Coal Science and Technology*, vol. 44, no. 11, pp. 160–166, 2016.

[11] D. Ren, L. Ma, D. Liu, J. Tao, X. Liu, and R. Zhang, "Control mechanism and parameter simulation of oil-water properties on spontaneous imbibition efficiency of tight sandstone reservoir," *Frontiers in Physics*, vol. 10, no. 10, p. 829763, 2022.

[12] P. Mou, J. Pan, Q. Niu, Z. Wang, Y. Li, and D. Song, "Coal pores: methods, types, and characteristics," *Energy & Fuels*, vol. 35, no. 9, pp. 7467–7484, 2021.

[13] D. Ren, H. Zhang, Z. Wang, B. Ge, D. Liu, and R. Zhang, "Experimental study on microscale simulation of oil accumulation in sandstone reservoir," *Frontiers in Physics*, vol. 10, no. 10, p. 841989, 2022.

[14] C. León, "New perspectives in mercury porosimetry," *Advances in Colloid and Interface Science*, vol. 76-77, pp. 341–372, 1998.

[15] W. I. Friesen and R. J. Mikula, "Fractal dimensions of coal particles," *Journal of Colloid and Interface Science*, vol. 120, no. 1, pp. 263–271, 1987.

[16] Z. Ye, E. Hou, and Z. Duan, "Micrometer-scale pores and fractures in coals and the effects of tectonic deformation on permeability based on fractal theory," *AIP Advances*, vol. 10, no. 2, article 025118, 2020.

[17] H. Xie, J. Wang, and P. Qan, "Fractal characters of micropore evolution in marbles," *Physics Letters A*, vol. 218, no. 3-6, pp. 275–280, 1996.

[18] B. Zhang, W. Liu, and X. Liu, "Scale-dependent nature of the surface fractal dimension for bi- and multi- disperse porous solids by mercury porosimetry," *Applied Surface Science*, vol. 253, no. 3, pp. 1349–1355, 2006.

[19] B. B. Hodot, *Outburst of Coal and Coalbed Gas*, China Industry Press, Beijing, 1966.

[20] F. Chen, Y. Ju, X. Li, D. Fan, and Y. Liang, "Diffusion-osmosis characteristics of coalbed methane in tectonically deformed coals and their mechanism," *Earth Science Frontiers*, vol. 17, no. 1, pp. 195–201, 2010.

[21] J. Cai, Z. Zhang, W. Wei, D. Guo, S. Li, and P. Zhao, "The critical factors for permeability-formation factor relation in reservoir rocks: Pore-throat ratio, tortuosity and connectivity," *Energy*, vol. 188, Article ID 116051, 2019.

[22] Q. Hu, Y. Zhang, X. Meng, Z. Li, Z. Xie, and M. Li, "Characterization of micro-nano pore networks in shale oil reservoirs of Paleogene Shahejie Formation in Dongying Sag of Bohai Bay Basin, East China," *Petroleum Exploration and Development*, vol. 44, no. 5, pp. 681–690, 2017.

[23] W. Zeng, Z. Song, and G. Zhou, "Pore structure of Qingshankou formation shales in Songliao basin and its geological significance," *Journal of China University of Petroleum (Edition of Natural Science)*, vol. 45, no. 6, pp. 35–41, 2021.

[24] Z. Huang, C. Jianping, X. Haitao, W. Yijun, W. Min, and D. Chunping, "Microstructural characteristics of the cretaceous Qingshankou formation shale, Songliao basin," *Petroleum Exploration and Development*, vol. 40, no. 1, pp. 61–68, 2013.

[25] N. C. Wardlaw and M. Mckellar, "Mercury porosimetry and the interpretation of pore geometry in sedimentary rocks and artificial models," *Powder Technology*, vol. 29, no. 1, pp. 127–143, 1981.

[26] M. Wang, J. Yang, Z. Wang, and S. Lu, "Nanometer-scale pore characteristics of lacustrine shale, Songliao basin, NE China," *PLoS One*, vol. 10, no. 8, article 0135252, 2015.

[27] M. Bao and H. Xu, "Study on oil-rich coal carbonization technology," *Coal processing & comprehensive utilization*, vol. 4, pp. 62–66, 2014.

[28] Z. Feng and Y. Zhao, "Pyrolytic cracking in coal: meso-characteristics of pore and fissure evolution observed by micro-CT," *Journal of China Coal Society*, vol. 40, no. 1, pp. 103–108, 2015.

[29] Z. Wang, Y. Cheng, Y. Qi, R. Wang, L. Wang, and J. Jiang, "Experimental study of pore structure and fractal characteristics of pulverized intact coal and tectonic coal by low temperature nitrogen adsorption," *Powder Technology*, vol. 350, pp. 15–25, 2019.

[30] E. M. Suuberg, S. C. Deevi, and Y. Yun, "Elastic behaviour of coals studied by mercury porosimetry," *Fuel*, vol. 74, no. 10, pp. 1522–1530, 1995.

[31] W. I. Friesen and O. I. Ogunsola, "Mercury porosimetry of upgraded western Canadian coals," *Fuel*, vol. 74, no. 4, pp. 604–609, 1995.

[32] M. Mahamud, Ó. López, J. J. Pis, and J. A. Pajares, "Textural characterization of chars using fractal analysis," *Fuel Processing Technology*, vol. 86, no. 2, pp. 135–149, 2004.

[33] B. Zhang and S. Li, "Determination of the surface fractal dimension for porous media by mercury porosimetry," *Industrial & Engineering Chemistry Research*, vol. 34, no. 4, pp. 1383–1386, 1995.